vation by catastrophic floods (*29*). After this initial flood, possible later flows would have been smaller discharges of Eridania lake subbasin A (Fig. 1A).

References and Notes

1. N. A. Cabrol, E. A. Grin, *Icarus* **142**, 160 (1999).
2. W. K. Hartmann, G. Neukum, *Space Sci. Rev.* **96**, 165 (2001).
3. R. P. Irwin III, A. D. Howard, *J. Geophys. Res.*, in press.
4. J. A. Grant, *Geology* **28**, 223 (2000).
5. R. D. Forsythe, C. R. Blackwelder, *J. Geophys. Res.* **103**, 31421 (1998).
6. T. J. Parker, S. M. Clifford, W. B. Banerdt, *Lunar Planet. Sci. Conf.* **31**, 2033 (2000).
7. T. J. Parker, R. S. Saunders, D. M. Schneeberger, *Icarus* **82**, 111 (1989).
8. J. W. Head III *et al.*, *Science* **286**, 2134 (1999).
9. D. E. Wilhelms, R. J. Baldwin, *Proc. Lunar Planet. Sci. Conf.* **19**, 355 (1989).
10. R. P. Sharp, M. C. Malin, *Geol. Soc. Am. Bull.* **86**, 593 (1975).
11. N. A. Cabrol, E. A. Grin, R. Landheim, *Icarus* **132**, 362 (1998).
12. N. A. Cabrol, E. A. Grin, G. Dawidowicz, *Icarus* **125**, 455 (1997).
13. D. E. Smith *et al.*, *J. Geophys. Res.* **106**, 23689 (2001).
14. G. D. Thornhill *et al.*, *J. Geophys. Res.* **98**, 23581 (1993).
15. N. A. Cabrol, E. A. Grin, G. Dawidowicz, *Icarus* **123**, 269 (1996).
16. J. E. O'Connor, *Geol. Soc. Am. Spec. Pap. 274* (1993).
17. N. A. Cabrol, E. A. Grin, R. Landheim, R. O. Kuzmin, R. Greeley, *Icarus* **133**, 98 (1998).
18. M. H. Carr, *Water on Mars* (Oxford Univ. Press, New York, 1996).
19. D. H. Scott, K. L. Tanaka, *U.S. Geol. Surv. Misc. Invest. Ser. Map I-1802-A* (1986).
20. R. Greeley, J. E. Guest, *U.S. Geol. Surv. Misc. Invest. Ser. Map I-1802-B* (1987).
21. R. A. Craddock, T. A. Maxwell, A. D. Howard, *J. Geophys. Res.* **102**, 13321 (1997).
22. A. D. Howard, *Eos* **81** (fall meet. suppl.), abstract P62C-06 (2000).
23. M. C. Malin, K. S. Edgett, *Science* **288**, 2330 (2000).
24. L. S. Manent, F. El-Baz, *Earth Moon Planets* **34**, 149 (1986).
25. H. V. Frey, K. M. Shockey, J. H. Roark, E. L. Frey, S. E. H. Sakimoto, 2001 GSA Annual Meeting, Boston, MA, 5 to 8 November 2001 (abstract 25358).
26. K. L. Tanaka, *J. Geophys. Res.* **91**, E139 (1986).
27. M. H. Carr, *J. Geophys. Res.* **84**, 2995 (1979).
28. P. D. Komar, *Icarus* **42**, 317 (1980).
29. B. L. Carter, H. Frey, S. E. H. Sakimoto, J. Roark, *Lunar Planet. Sci. Conf.* **32**, 2042 (2001).

30. Supported by NASA grants NAG5-3932 and NAG5-9817.

2 February 2002; accepted 3 May 2002

The Mass Disruption of Oort Cloud Comets

Harold F. Levison,[1]* Alessandro Morbidelli,[2] Luke Dones,[1] Robert Jedicke,[3] Paul A. Wiegert,[4] William F. Bottke Jr.[1]

We have calculated the number of dormant, nearly isotropic Oort cloud comets in the solar system by (i) combining orbital distribution models with statistical models of dormant comet discoveries by well-defined surveys and (ii) comparing the model results to observations of a population of dormant comets. Dynamical models that assume that comets are not destroyed predict that we should have discovered ~100 times more dormant nearly isotropic comets than are actually seen. Thus, as comets evolve inward from the Oort cloud, the majority of them must physically disrupt.

It has been over half a century since Jan Oort first argued that a roughly spherical cloud of comets, which extends to heliocentric distances larger than 100,000 astronomical units (AU), surrounds the solar system (*1*). This structure, which is now known as the Oort cloud, is currently feeding comets into the inner solar system (with perihelion distances, q, of less than 3 AU) at a rate of about 12 comets per year with an active comet absolute magnitude, H_{10}, <10.9 (*2*, *3*). These comets as a whole are known as nearly isotropic comets (NICs) (*4*). NICs can be divided into the following two subpopulations, based on their dynamical histories (*5*): (i) dynamically new NICs, which are on their first pass through the system and typically have semi-major axes, a, greater than ~10,000 AU, and (ii) returning NICs, which have previously passed through the inner solar system and typically have $a \leq 10{,}000$ AU.

One unsolved problem is that models of the orbital evolution of new NICs into returning NICs consistently predict many times more returning comets than are observed (*2*, *6*). This so-called "fading problem" cannot be due to previously unmodeled dynamical effects (*2*) and thus must be due to the physical evolution of the comets' activity (*7*). An important issue, therefore, is to determine the fate of the missing comets; either they become extinct or dormant (*8*), or they disintegrate entirely (*9*, *10*). Here, we try to distinguish between these two possible outcomes by comparing model results to observations of dormant comets.

Large ground-based surveys have discovered 11 asteroidal objects, as of 3 December 2001, that are on orbits consistent with active NICs with $q < 3$ AU (Table 1) (*11*) [see supporting online material (SOM)]. These 11 objects represent just a small fraction of the total population of dormant NICs, because ground-based surveys suffer from unavoidable observational biases (*12*). Thus, the main purpose of the work presented here is to estimate the total number of dormant NICs based on the available data. We accomplish this by the following steps: (i) we use numerical simulations of cometary dynamics to produce a set of fictitious dormant NICs, (ii) we run these fictitious NICs through a near-Earth object (NEO) survey simulator to determine which ones would be discovered, and (iii) we compare the results of (ii) to observations of the known dormant NICs to estimate the total number and orbital element distribution of the entire real dormant NIC population.

We determined the expected orbital element distribution for the dormant NICs from long-term dynamical simulations that track thousands of fictitious new comets entering the planetary system from the Oort cloud for the first time. The simulations calculate the dynamical evolution of these objects' orbits caused by the gravitational influence of the Sun, planets, and Milky Way Galaxy. The objects' trajectories are followed until they are either ejected from the solar system, hit a planet, or strike the Sun. From this, we can develop a steady-state distribution of NICs by assuming that the influx rate of dynamically new comets is constant with time.

We used simulations that were performed elsewhere (*2*, *13*). Because of differing computational challenges, these simulations have

Table 1. Known dormant NICs.

Asteroid Desig.	a (AU)	e	i (Deg)	q (AU)	H
(15504) 1999 RG_{33}	9.4	0.77	35	2.1	12.1
2000 DG_8	10.8	0.79	129	2.2	12.8
(5335) Damocles	11.8	0.87	62	1.6	13.3
2001 OG_{108}	13.3	0.93	80	1.0	13.0
1998 WU_{24}	15.2	0.91	43	1.4	15.0
1999 XS_{35}	18.0	0.95	19	0.95	17.2
(20461) 1999 LD_{31}	24.0	0.90	160	2.4	13.8
2000 HE_{46}	24.0	0.90	158	2.4	14.6
1997 MD_{10}	26.7	0.94	59	1.5	16.0
2000 AB_{229}*	52.5	0.96	69	2.3	14.0
1996 PW*	287	0.99	30	2.5	14.0

The columns are: Desig., designation; a, semi-major axis; e, eccentricity; i, inclination; q, perihelion distance; and H, Absolute Magnitude. See text for definitions. *All are type HTC, except the last two, which are ERCs.

[1]Southwest Research Institute, 1050 Walnut Street, Suite 426, Boulder, CO 80302, USA. [2]Observatoire de la Cote d'Azur, B. P. 4229, 06034 Nice Cedex 4, France. [3]Lunar and Planetary Laboratory, University of Arizona, Tucson, AZ 85721, USA. [4]Department of Physics, Queen's University, Kingston, Ontario K7L 3N6, Canada.

*To whom correspondence should be sent. E-mail: hal@gort.boulder.swri.edu

divided returning NICs into two subclasses: external returning comets (ERCs) with periods greater than 200 years, and Halley-type comets (HTCs) with orbital periods less than 200 years (*14*, *15*).

We used Wiegert and Tremaine's model (*2*) to determine the orbital element distribution that dormant ERCs would have if there were no disruptions. We also adopted the standard form for the cumulative absolute magnitude, H, distribution of $N(<H) \propto 10^{\alpha H}$ (*16*–*18*), where N is the total number of objects brighter than H and α is the slope of the H distribution. We set $\alpha = 0.28$. This value of α is determined directly from our models of the HTCs, which are described below. It is much smaller (or the H distribution is much shallower) than is typically assumed. However, it is consistent with a recent observational study of active comets (*19*).

With the above distribution of ERCs, we then used a survey simulator described in (*20*) to determine which objects would be discovered by modern NEO surveys. The survey simulator discovered 1 out of every 22,000 dormant ERCs with $q < 3$ AU and $H < 18$ (*21*) in Wiegert and Tremaine's model (*2*). This result, combined with the fact that only 2 dormant ERCs actually have been discovered thus far (Table 1) (also see SOM), implies that there are a total of 44,000 ± 31,000 dormant ERCs that are brighter than $H = 18$ and have a $q < 3$ AU in the solar system (*22*).

The ERCs have orbital periods that are so long that it is traditional to express the population numbers in terms of the number of objects that pass through perihelion per year. Based on the two objects thus far discovered and the mean inverse orbital period of objects in Wiegert and Tremaine's model (*2*), we estimate that there should be 3.9 ± 2.7 dormant ERCs with $H < 18$ and $q < 3$ AU passing perihelion per year. Assuming no disruptions, Wiegert and Tremaine's model predicts that there should be ~400 dormant ERCs with $q < 3$ AU passing perihelion per year (see SOM). The discrepancy between our estimate based on observing dormant NICs and the one based on dynamics alone implies that, when a comet becomes inactive, it only has a ~3.9/400, or 1%, chance of becoming dormant. We can only conclude that the other ~99% of these objects must have disrupted.

To perform these calculations, we assumed a value of $\alpha = 0.28$. We must therefore estimate how this choice affects our result concerning the disruption of ERCs. Previous estimates of α have ranged from 0.28 to 0.53 (*23*). As we discussed above, if we assume that $\alpha = 0.28$, our survey simulator discovers 1/22,000 of the dormant ERCs with $H < 18$. If α were 0.53, our survey simulator would discover 1/43,000 of these objects, which is only a factor of 2 different from the $\alpha = 0.28$ result. Thus, changing α does not change our conclusion that ~99% of the inactive ERCs disrupt.

We now turn our attention to the HTCs. Levison *et al*. (*13*) studied the dynamical evolution of comets from the Oort cloud into HTC-like orbits (restricting themselves to HTCs with $q < 2.5$ AU). As with the ERCs, Levison *et al*. found a significant fading problem with the HTCs. In particular, Levison *et al*.'s models predict that there should be more than 15,000 active HTCs in the solar system, whereas the debiased estimate of active HTCs based on the observed population would suggest that there are only 50 (*13*). Thus, they concluded that ≥99% of these comets disappeared.

To determine whether HTCs become dormant or disrupt, we compare a model of dormant HTC discoveries (i.e., we take the results of dynamical models with no disruption and run them through our survey simulator) to actual discoveries. If we adopt Levison *et al*.'s models unaltered (see SOM), we are unable to construct models of the dormant HTC population that are consistent with observations (Fig. 1). Although the models produce reasonable inclination distributions (Fig. 1D), they fail to reproduce the observed semi-major axis distribution (Fig. 1C). In particular, the models predict a far larger number of dormant HTCs with $a < 10$ AU than has been observed.

One reason Levison *et al*.'s model fails could be that it does not adequately account for the fact that comets suffering a close encounter with the Sun are more likely to disrupt than are comets that have larger perihelion distances. Thus, we added a q-sensitive disruption law (*24*) to Levison *et al*.'s model and assumed that the absolute magnitude power law index is $\alpha = 0.28$ (as before). We then recalculated Levison *et al*.'s fitting procedures and determined the model that provides the best fit to both the active and dormant HTC populations (see SOM). This

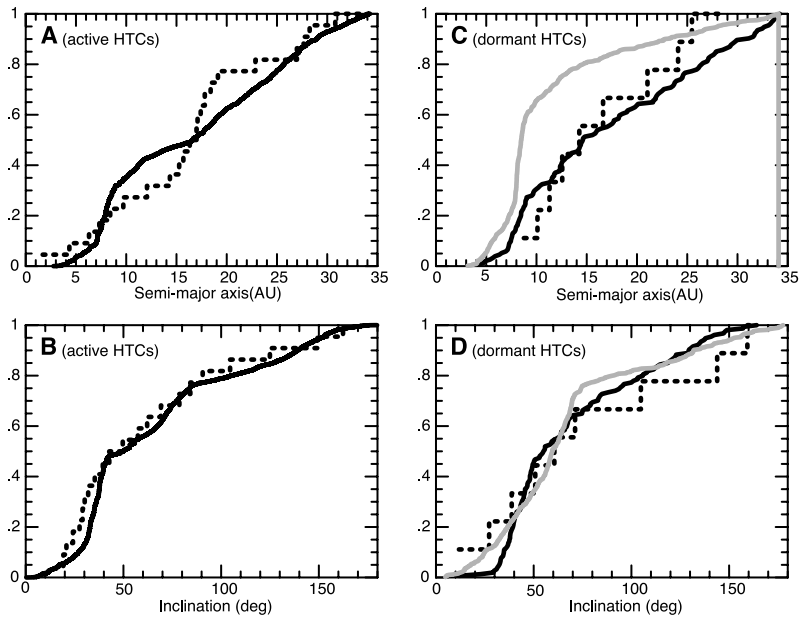

Fig. 1. The cumulative semi-major axis (*a*) distribution (**A** and **C**) and inclination distribution (**B** and **D**) for observed active HTCs (A) and (B) and dormant HTCs (C) and (D). The dotted curves represent the real objects observed in the solar system. The gray curves show the distributions of dormant comets as predicted by processing the unbiased best-fit dynamic model through our survey simulator [see (*13*) for the distribution of active comets]. The black curves show these distributions for our best-fit model.

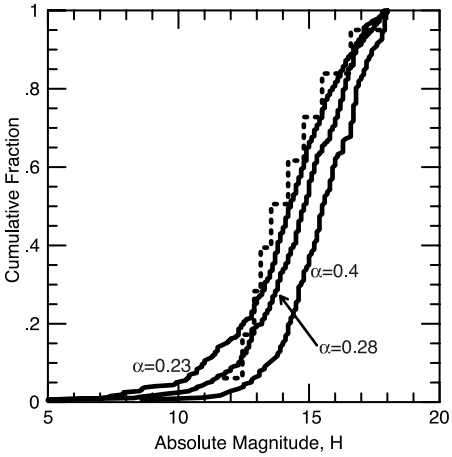

Fig. 2. The cumulative absolute magnitude (H) distribution of dormant HTCs discovered by NEO surveys. The dotted curve represents the real objects. The solid curves show the distribution predicted by our best-fit model for three different values of α (0.23, 0.28, and 0.4).

model shows good agreement with the observations (Fig. 1).

Up to this point, we have been assuming a value of α. We could not determine α for the ERC simulations because there are only two known dormant ERCs. There are enough known dormant HTCs (nine of them), however, to estimate α directly. The cumulative absolute magnitude distribution (*25*) for the observed dormant HTCs is clearly inconsistent with those detected by our survey simulator for values of α as large as 0.4 (Fig. 2). Indeed, the probability that the observed and modeled absolute magnitude distributions are drawn from the same parent distribution (fig. S2) shows that we can rule out any α larger than $\sim$0.35 and that the best fit is $\alpha = 0.23 \pm 0.04$ (1σ). We decided to adopt Weissman and Lowry's (*19*) value of 0.28 because it is consistent with our results and yet is based on a larger data set. The differences between models using $\alpha = 0.28$ and $\alpha = 0.23$ are small, and thus this choice will not measurably affect our results.

With $\alpha = 0.28$, the survey simulator discovers 1.1% of the dormant HTCs. Given that the NEO surveys have discovered 9 dormant HTCs (Table 1), we conclude that there are 780 ± 260 dormant HTCs in the solar system with $H < 18$ and $q < 2.5$ AU.

We can now compare our estimate of the number of dormant HTCs to what we would expect from dynamical models, assuming no disruption (*26*). Our model predicts that there should be 46,000 active and dormant HTCs with $q < 1.3$ AU, which implies $\sim$106,000 with $q < 2.5$ AU. Because dormant comets far outnumber active comets (*27*), we can conclude that $\sim$99% of ERCs disrupt before becoming HTCs. This percentage is similar to the fraction predicted for the ERCs alone.

Jupiter-family comets (JFCs) do not appear to disrupt at the same rate (*28*) as do the NICs. Bottke *et al*. (*29*) estimated the total number of dormant JFCs from the known population of NEOs, finding that there are 61 ± 43 dormant JFCs with $q < 1.3$ AU and $H < 18$. This number is consistent with estimates from dynamical simulations, assuming that all objects become dormant rather than disrupt [$\sim 60^{+40}_{-53}$% become dormant (*30*)]. Despite large uncertainties in this estimate, it is clear that a substantial fraction of JFCs must become dormant, and thus they behave differently from NICs (see SOM for additional arguments).

It is surprising that NICs and JFCs behave so differently, because they are thought to be composed of similar mixtures of ice and rock. Their different disruption behaviors could be primordial, reflecting the chemical or physical characteristics of their formation locations. Most Oort cloud comets are believed to have formed in the region of the giant planets (*1*, *31*), whereas JFCs are thought to have formed in the Kuiper belt beyond the giant planets (*32*–*34*). However, recent simulations of Oort cloud formation (*35*) suggest that $\sim$30% of the present-day Oort cloud originated in the Kuiper belt (although most of these objects left the Kuiper belt a long time ago). If these models are correct, then the different disruption behaviors cannot stem from primordial differences, because the fraction of NICs that originated in the Kuiper belt is far larger than the $\sim$1% that avoid disruption.

Alternatively, evolutionary processes could affect comets' susceptibility to disruption. For example, over long time scales, Kuiper belt comets could have lost more volatiles than did Oort cloud comets because Kuiper belt comets have been stored at closer heliocentric distances and thus higher temperatures. Kuiper belt objects could be more porous, and thus less susceptible to disruption resulting from volatile pressure buildup, due to a relatively violent collisional environment (*36*). Finally, the dynamical pathways that NICs and JFCs take on their way into the inner solar system might lead to different thermal histories for the two populations. In one orbital period, most NICs evolve from distant orbits (with perihelia outside the planetary region) to orbits that closely approach the Sun. On the other hand, objects from the Kuiper belt slowly move through the planetary region, taking $\sim$10 million years to evolve onto orbits with $q < 2.5$ AU (*33*). It has been argued previously (*37*) that different thermal histories could lead to different disruption rates, so perhaps NICs disrupt because of strong thermal gradients or volatile pressure buildup, whereas JFCs survive because they are warmed more slowly.

References and Notes

1. J. H. Oort, *Bull. Astron. Inst. Neth.* **11**, 91 (1950).
2. P. Wiegert, S. Tremaine, *Icarus* **137**, 84 (1999).
3. H_{10} is a distance-independent measure of the brightness of active comets that includes the coma.
4. We use the notation of (*14*). An NIC is defined as an object that has a Tisserand parameter, *T*, with respect to Jupiter, of less than 2. The encounter velocity with Jupiter is $v_J\sqrt{3-T}$, where v_J is the mean orbital velocity of Jupiter around the Sun. NICs typically have semi-major axes greater than that of Jupiter.
5. On their first trip through the inner solar system, NICs have semi-major axes, *a*, larger than $\sim$10,000 AU. The large *a*'s result from the dynamics of the Oort cloud itself. Oort cloud comets are brought into the planetary region by the gravitational effects of the Galaxy, which act like a tide. The tide grows larger as a comet moves farther from the Sun. Objects initially on orbits with $a < 10{,}000$ AU rarely make it directly into the inner solar system because they first gravitationally encounter a giant planet [see (*31*, *38*) for a more complete discussion]. However, beyond $\sim$10,000 AU, the tides are strong enough that a comet can effectively jump over the jovian planet region (i.e., the comet's perihelion distance, *q*, can evolve from $\geq$10 to $\leq$3 AU in just one orbital period). Thus, it can arrive in the inner solar system without being measurably perturbed by a giant planet. Once comets are in the inner planetary system for the first time, gravitational interactions with the giant planets can then either eject them from the solar system entirely or markedly alter their semi-major axes from $a > 10{,}000$ AU to much smaller values. (*1*, *9*, *39*). Thus, comets that have made more than one passage through the planetary system, which are called returning comets, typically have smaller semi-major axes than do those on their first passage.
6. P. R. Weissman, *Astron. Astrophys.* **85**, 191 (1980).
7. NICs are the brightest and most active during their first few passages through the planetary system and then disappear before subsequent passages [see (*2*) and references therein].
8. A comet becomes extinct if it loses all its volatiles. It becomes dormant if, as a result of its passages through the planetary system, a lag deposit of inert material builds up over its entire surface (*40*, *41*). Such mantles have been observed to cover large fractions of the two comets that have been imaged in detail by spacecraft flybys [i.e., 1P/Halley (*42*), which is an NIC, and 19P/Borrelly (*43*)]. A dormant comet can become active again if its mantle is disturbed. In this paper, we do not take this reactivation into account. We also do not distinguish between dormant and extinct comets and we henceforth refer to both states as dormant.
9. P. R. Weissman, in *Dynamics of the Solar System*, *IAU Symposium 81*, R. L. Duncombe, Ed. (Reidel, Dordrecht, Netherlands, 1979), pp. 277–282.
10. Such events are known to happen, as illustrated by the spectacular disruption of comet C/1999 S4 (LINEAR) (*44*). See http://oposite.stsci.edu/pubinfo/PR/2000/27/ for images taken with the Hubble Space Telescope.
11. Dormant comets will look like asteroids because they lack, by definition, any cometary activity. Thus, they are classified as asteroids by the International Astronomical Union and are given asteroid designations. However, physically they still are dormant comets.
12. R. Jedicke, J. Larsen, T. Spahr, in *Asteroids III*, W. F. Bottke, A. Cellino, P. Paolicchi, R. Binzel, Eds., (Univ. Arizona Press, Tucson, AZ, in press).
13. H. F. Levison, L. Dones, M. J. Duncan, *Astron. J.* **121**, 2253 (2001).
14. H. F. Levison, in *Completing the Inventory of the Solar System*, T. W. Rettig, J. M. Hahn, Eds. (Astronomical Society of the Pacific, San Francisco, 1996), pp. 173–192.
15. HTCs have small enough semi-major axes that planetary–mean motion resonances can play a role in their evolution (*45*). These resonances are unimportant for external returning comets or ERCs. Hence, external implies that the comet is beyond the region where resonances are important. For our purposes, this distinction is made for historical and numerical reasons. As comets evolve out of the Oort cloud, a larger fraction become ERCs than become HTCs, so the study of these two NIC subclasses requires different numerical techniques. Wiegert and Tremaine (*2*) studied only ERCs, whereas Levison *et al*. (*13*) studied the HTCs alone. We treat these two studies separately.
16. E. Everhart, *Astron. J.* **72**, 1002 (1967).
17. D. W. Hughes, *Mon. Not. R. Astron. Soc.* **326**, 515 (2001).
18. This absolute magnitude distribution is equivalent to a differential size distribution that is also a power law of the form $dN/dD \propto D^{-(5\alpha + 1)}$, where *D* is an object's diameter. A collisional equilibrium corresponds to $\alpha = 0.5$.
19. P. R. Weissman, S. C. Lowry, *Bull. Am. Astron. Soc.* **33**, 1094 (2001).
20. R. Jedicke, A. Morbidelli, T. Spahr, J.-M. Petit, W. Bottke, *Icarus*, in press.
21. Our brightness limit is somewhat arbitrary. We chose it because it is the next integer fainter than the faintest object in Table 1, which has $H = 17.2$. Assuming an albedo of 2% (*46*), an $H = 18$ object has a diameter of 2.4 km.
22. Our quoted error is 1σ. We calculated it assuming Poisson statistics using the two objects thus far discovered.
23. The classic measurement is by (*47*), who estimated α using the size distribution of craters on the Galilean satellites of Jupiter. More recent measurements using the observed magnitudes of comets far from the Sun are $\alpha = 0.53 \pm 0.05$ (*48*), 0.32 ± 0.02 (*49*), and

0.28 ± 0.03 (*19*). The measurements of α using cometary nuclei need to be viewed with caution, because they are observationally challenging, and so the measurements could have problems. For example, measurements of individual comets could have been performed when there was still some small amount of cometary activity—too small to resolve but large enough to affect the photometry. In addition, all objects studied in these surveys are bright active comets when observed near perihelion, which could introduce biases in the way they were selected. What is clearly needed is a population of dormant objects whose members were discovered in a systematic way. The data set studied here supplies us with such a population.

24. Levison *et al*. assume that active comets fade in brightness over many orbits after they reach $q < 2.5$ AU. However, they do not distinguish between close (say, $q \sim 0.5$ AU) and distant (say, $q \sim 2.5$ AU) passages. We believe, however, that closer perihelion passages lead to increased damage to comets. For this reason, we have added an additional disruption law to Levison *et al*.'s models. This simple law is designed to mimic the q dependence of fading, while making the fewest changes to the original Levison *et al*.'s models. If an object evolves onto an orbit with $q < 1$ AU, we assume that it has a 96% chance of disrupting before its next perihelion passage (see SOM). If the comet disrupts, it will not appear in either the active comet or dormant comet populations.
25. Fortunately, the *a*–*i* distribution (i.e., semi-major axis and inclination) of our models is not sensitive to α, so we can perform the absolute magnitude fitting procedure on our best-fit model alone. In particular, we do not need to perform a calculation that varies the four parameters from (*13*) and α, while fitting to *a*, *i*, and *H* simultaneously.
26. To do this comparison, we use arguments developed in (*13*) for relating the observed number of dynamically new comets per year to the total number of HTCs.
27. There are 22 known active HTCs with $q < 1.3$ AU (a limit set by observational biases), although not all HTCs with $q < 1.3$ AU have yet been discovered. We can predict the total number of active HTCs with our dynamical models. Our best-fit model for the HTCs predicts 84 active HTCs with $q < 1.3$ AU. This value, in turn, implies that there are 194 active HTCs with $q < 3$ AU.
28. JFCs are comets with Tisserand parameters $2 < T \leq 3$ [see (*4*, *14*)]. These objects are believed to arise in the Kuiper belt (*32*, *33*) or the scattered disk (*34*)—not in the Oort cloud.
29. W. F. Bottke Jr. *et al.*, *Icarus* **156**, 399 (2002).
30. From results given in (*48*), we estimate that there are 30^{+10}_{-5} active JFCs with $H < 18$ and $q < 1.3$ AU. From (*33*), for each active comet, there should be between 2.0 and 6.7 dormant comets, with a best-fit value of 3.5. This assumes no disruption. Thus, we estimate that the total number of dormant JFCs with $H < 18$ and $q < 1.3$ AU is $30 \times 3.5 = 105$, with a possible range of 50 to 268, if all inactive comets become dormant. Given Bottke's (*29*) estimate of dormant JFCs from the NEO surveys (61 with $H < 18$), our best estimate is that 61/105, or ~60%, of the JFCs become dormant, as opposed to ≤1% of the NICs. Formally, the fraction of JFCs that become dormant could be as small as 7% or as large as 100%. Even the lower limit is about an order of magnitude larger than our upper limit for the fraction of NICs that become dormant.
31. M. Duncan, T. Quinn, S. Tremaine, *Astron. J.* **94**, 1330 (1987).
32. _____, *Astrophys. J. Lett.* **328**, 69 (1988).
33. H. F. Levison, M. J. Duncan, *Icarus* **127**, 13 (1997).
34. M. J. Duncan, H. F. Levison, *Science* **276**, 1670 (1997)
35. L. Dones, H. F. Levison, M. J. Duncan, P. R. Weissman, *Am. Astron. Soc. Div. Dynamical Astron. Meeting* **32**, 1103 (2001).
36. The Kuiper belt is currently collisionally active (*50*), whereas the Oort cloud is not.
37. M. Bailey, *Mon. Not. R. Astron. Soc.* **221**, 247 (1984).
38. J. G. Hills, *Astron. J.* **86**, 1730 (1981).
39. F. L. Whipple, *Astron. J.* **67**, 1 (1962).
40. G. D. Brin, D. A. Mendis, *Astrophys. J.* **229**, 402 (1979).
41. D. Prialnik, A. Bar-Nun, *Icarus* **74**, 272 (1988).
42. H. U. Keller *et al.*, *Nature* **321**, 320 (1986).
43. L. Soderblom *et al.*, *Science* **296**, 1087 (2002).
44. H. Boehnhardt, *Science* **292**, 1307 (2001).
45. J. Chambers, *Icarus* **125**, 32 (1997).
46. Y. R. Fernández, D. C. Jewitt, S. S. Sheppard, *Astrophys. J. Lett.* **553**, L197 (2001).
47. E. M. Shoemaker, R. F. Wolfe, in *Satellites of Jupiter*, D. Morrison, Ed. (Univ. Arizona Press, Tucson, AZ, 1982), pp. 277–339.
48. J. A. Fernández, G. Tancredi, H. Rickman, J. Licandro, *Astron. Astrophys.* **352**, 327 (1999).
49. S. C. Lowry, thesis, Queen's University, Belfast, UK (2001).
50. S. A. Stern, J. E. Colwell, *Astrophy. J.* **490**, 879 (1997).
51. We thank M. Duncan, S. A. Stern, and P. Weissman for useful discussions and comments on an early draft of this paper; and M. Bailey for useful comments on this manuscript. H.L., W.B., and L.D. acknowledge support from NASA's Planetary Geology and Geophysics (NAG5-9479, NAG5-10331, NAG5-9141), Origins of Solar Systems (NAG5-10661), NEO-Observations (NAG5-9951), and Mars-Data Analysis (NAG5-10603) programs. A.M. was subsidized by European Space Agency contract 14018/2000/F/TB. Travel support provided by grants from NATO and NSF/Centre National de la Recherche Scientifique. Observations by Spacewatch and research by R.J. supported by grants from NASA (NAG5-7854, NAG5-10447, NAG5-7533), the Air Force Office of Scientific Research (F49620-00-1-0126), the David and Lucile Packard Foundation, the Steven and Michele Kirsch Foundation, the Paul G. Allen Charitable Foundation, and other contributors.

Supporting Online Material

www.sciencemag.org/cgi/content/full/296/5576/2212/DC1
Materials and Methods
Figs. S1 and S2
References and Notes

25 January 2002; accepted 3 April 2002

Identification of Signal Peptide Peptidase, a Presenilin-Type Aspartic Protease

Andreas Weihofen,[1] Kathleen Binns,[2] Marius K. Lemberg,[1] Keith Ashman,[2] Bruno Martoglio[1]*

Signal peptide peptidase (SPP) catalyzes intramembrane proteolysis of some signal peptides after they have been cleaved from a preprotein. In humans, SPP activity is required to generate signal sequence–derived human lymphocyte antigen–E epitopes that are recognized by the immune system, and to process hepatitis C virus core protein. We have identified human SPP as a polytopic membrane protein with sequence motifs characteristic of the presenilin-type aspartic proteases. SPP and potential eukaryotic homologs may represent another family of aspartic proteases that promote intramembrane proteolysis to release biologically important peptides.

The discovery of intramembrane proteolysis has revealed alternative pathways in cell signaling, cell regulation, and protein processing (*1*). Dormant, membrane-bound transcription factors, like sterol regulatory element–binding protein (*1*), activating transcription factor–6 (*2*), and NOTCH (*3*), or the growth factor Spitz in *Drosophila* (*4*), are activated and liberated in regulated processes that culminate in proteolytic cleavage within their membrane anchor. Similarly, β-amyloid (Aβ) peptides, which are believed to be the main toxic component in Alzheimer's disease, are generated from membrane-anchored β-amyloid precursor protein (β-APP) (*5*). The critical cleavage in the membrane anchor of β-APP is thought to be catalyzed by the aspartic protease presenilin (*6*).

Processing of signal peptides by an SPP is related to protein cleavage by presenilin. Both proteases cleave their substrates within the center of a transmembrane region (*6*, *7*). The discovery of posttargeting functions of signal peptides, which are required primarily for the biosynthesis of secretory and membrane proteins, has pointed to a central role for SPP activity (*8*). Generation of cell surface histocompatibility antigen (HLA)–E epitopes in humans requires processing of signal peptides by SPP (*9*). HLA-E epitopes originate from the signal sequence of polymorphic major histocompatibility complex (MHC) class I molecules and report biosynthesis of these molecules to the immune system (*10*). SPP activity is also required for processing hepatitis C virus polyprotein and hence is exploited by the pathogen to produce viral components (*11*). It is thought that SPP promotes the liberation of functional signal peptide fragments from the endoplasmic reticulum (ER) membrane (*8*).

To identify human SPP, we synthesized a ligand affinity probe based on the SPP inhibitor $(Z\text{-LL})_2$–ketone, which is thought to re-

[1]Institute of Biochemistry, Swiss Federal Institute of Technology (ETH), ETH-Hoenggerberg, 8093 Zürich, Switzerland. [2]Samuel Lunenfeld Institute, Proteomics, 600 University Avenue, Toronto, Ontario M5G 1X5, Canada.

*To whom correspondence should be addressed. E-mail: bruno.martoglio@bc.biol.ethz.ch

Supplementary Online Information

Outline:

I. Surveys and Biases: Many of the asteroidal objects used in our analysis have been found by LINEAR, a Near-Earth Object (NEO) survey program capable of covering large areas of the sky each lunation [1]. Most of the remaining objects have been found by other NEO surveys with observing strategies and limiting magnitudes comparable to LINEAR (e.g., NEAT, LONEOS, and the Catalina Sky Survey).

These surveys suffer from significant observational biases that not only affect the number of objects that we see, but also the observed orbital element distribution. To illustrate how these biases work, we present an example of perhaps the most important bias. From Earth, the apparent brightness of an asteroidal object varies roughly as r^{-4}, where r is the heliocentric distance of the object. Dormant NICs typically have semi-major axes so large that the surveys employed here can only detect them when they are near perihelion. Thus, only those objects that pass perihelion during the time that the surveys were observing had a possibility of being discovered. Because the orbital periods of the dormant NICs are longer than the length of time the surveys were active (~ 30 to $\sim 10^6$ yrs vs. ~ 5 yrs), only a small fraction of the NICs could have been discovered. Complicating the issue even further, this fraction is a function of the NIC's semi-major axis.

Therefore, as part of our analysis, we employ a model of these surveys [2] that allows us to take a prediction of the actual population of comets, which is generated

by dynamical modeling, and produce a model of what we expect these surveys to see. The workers in [2] created a simple, and yet effective, model of the LINEAR survey that reproduces LINEAR's NEO discovery and re-discovery rates. The code models the LINEAR survey as covering the entire visible dark night sky from -30° to +80° declination on 14 nights centered on new moon every lunation. On each night $1/14^{th}$ of the sky is covered to a limiting V magnitude of 18.5 in a band of declination moving northwards as the lunation progresses. The simulator takes as input any orbit-absolute magnitude distribution and outputs a list of discovered objects found during the simulated survey. [2] argue that this code can be used to model all of the main NEO surveys since it provides a good match to the total number, orbital element distribution, and absolute magnitude distribution of the known NEOs from all these observatories discovered before 15 March 2001. This survey simulator is designed for asteroidal objects only and thus cannot be used for active comets.

One result of these observational biases is that the semi-major axis distribution of the observed dormant comets can be very different from the actual distribution. We find this to be particularly true for the ERCs. 1996 PW has $a = 287\,\mathrm{AU}$ and 2000 AB_{229} has $a = 52.5\,\mathrm{AU}$. These bodies have surprisingly small semi-major axes, given that WT99's model [3] has a median semi-major axis of $\sim 2500\,\mathrm{AU}$ (solid curve in Fig. S1). However, roughly 80% of the ERCs discovered by our survey simulator have semi-major axes less than that of 1996 PW, while $\sim 20\%$ have semi-major axes less than 2000 AB_{229} (see the dotted curve in Fig. S1). Thus, it seems reasonable that the two objects thus far discovered have the semi-major axes that they do.

There is one aspect of the surveys that has not been modeled by our survey simulator. An object that has a large drift rate with respect to the background stars will appear as a streak in the survey images. This streak smears the object's light out over more than one pixel, thereby reducing the limiting magnitude of the survey. The fraction of objects that are not discovered because of this smearing depends on the objects' absolute magnitude. This is because in order to be discovered, intrinsically faint objects (large H) must come closer to the Earth than intrinsically

bright objects (small H) and thus are more likely to streak.

This smearing effect was not included in our simulations because it is different for the various surveys that we are modeling. However, we can estimate its importance by looking at the drift rates of the objects that our survey simulator has discovered as a function of absolute magnitude. For example, take the LINEAR survey. LINEAR's CCDs have pixels that are 2.27" on a side. The maximum exposure used by LINEAR (during darktime at opposition) is 11 seconds. So smearing becomes important if an object's drift rate is larger than ~ 5 deg/day. We reran our ERC simulations by replacing our normal absolute magnitude distribution with a single absolute magnitude and calculated the fraction of objects discovered that had drift rates smaller than 5 deg/day (so there is no smearing). We found that this fraction is 0.91 and 0.82 for $H = 17$ and 18, respectively, and 0.07 and 0 for $H = 21$ and 22. So, we conclude that this effect is not significant in our calculations in the main text, which are restricted to objects with $H < 18$. However, we predict that the LINEAR survey should have a dramatically reduced efficiency for detecting objects on NIC-like orbits fainter than $H \sim 21$. We use this conclusion below.

II. Choosing Dormant NICs for Table 1: Table 1 lists 11 asteroidal objects that are on orbits consistent with active NICs with $q < 3$ AU that were discovered by ground-based observers before December 3, 2001. This list was compiled as follows. We searched the lists of 'Unusual Minor Planets' at the Minor Planet Center (http://cfa-www.harvard.edu/iau/lists/Unusual.html), which are updated daily, for bodies with Tisserand parameter $T < 2$ and $q < 3$ AU. This search yielded ten 'other unusual objects' (`http://cfa-www.harvard.edu/iau/lists/Others.html`) and one Apollo asteroid, 1999 XS_{35} (`http://cfa-www.harvard.edu/iau/lists/Apollos.html`).

Our list does not include a few weakly active NICs that were originally thought to be asteroidal but were found to be comets soon after their discovery (e.g. C/2000 OF_8 (Spacewatch), C/2001 HT_{50} (LINEAR-NEAT)). It does, however, contain 2001 OG_{108}, which appeared asteroidal when discovered in July 2001, but began displaying a coma in January 2002. We include this object because our simulation of

discovery refers to a specific period of time which predates the discovery of activity. For the same reason, our list does not contain the apparent dormant NIC, 2002 CE_{10}, which was discovered after December 3, 2001. And finally, note that (20461) 1999 LD_{31} and 2000 HE_{46} have very similar orbits and thus could be a single object that recently split. We consider these separate objects in our calculations. The ambiguities in exactly which objects to consider in our calculation introduces a factor of $\lesssim 2$ uncertainty in our estimate of the population of extinct NICs.

III. The Number of Dormant ERCs Predicted by WT99: We claim in the main body of the paper that, assuming no disruptions, WT99's model [3] predicts that there should be ~ 400 dormant ERCs with $q < 3\,\mathrm{AU}$ passing perihelion per year. This value, however, is not directly reported by WT99, but can be deduced from other numbers given. WT99 argue that there are 12 new comets per year passing perihelion within 3 AU with $H_{10} < 10.9$ (H_{10} is a distance-independent measure of the brightness of active comets that includes the coma). According to two relations that have been proposed, $H_{10} = 10.9$ corresponds to a cometary nuclear absolute magnitude of $H = 17.2$ [4] or $H = 19.2$ [5]. Assuming $\alpha = 0.28$, we can convert the number of comets with $H_{10} < 10.9$ to the number with $H < 18$, so we can compare directly with asteroids, by multipling by $10^{\alpha(17.2-18)} = 0.6$ [4] or $10^{\alpha(19.2-18)} = 2.2$ [5]. Given the large differences between these factors and the fact that the value 1 lies between them, we will adopt 1. Thus, we assume that 12 dynamically new comets with $H < 18$ pass perihelion within 3 AU per year. WT99's model also predicts 35 ERCs for each dynamically new comet. Thus, we conclude that there are $35 \times 12 = 420$ bodies passing perihelion within 3 AU per year. This value refers to both active and dormant NICs. There are 36 *active* NICs passing perihelion per year [3]. Thus, we deduce that in WT99's model there are $420 - 36 = 384$ extinct NICs passing perihelion per year with $q < 3\,\mathrm{AU}$ and $H < 18$. The uncertainties in the conversion between H_{10} and H allow for values between 216 and 888. We adopt ~ 400 and note that there is a roughly a factor of 2 uncertainty in this number.

IV. Details of LDD01's models: LDD01's models [6] are more complex than the WT99 models because, unlike the ERCs and dynamically new NICs that have nearly isotropic inclination distributions, the inclination distribution of the HTCs is flattened with a median inclination of 45°. LDD01 show that the most likely explanation for this is that the inner parts of the Oort cloud are likewise flattened. However, the only constraint on this structure is the orbits of the HTCs themselves.

Thus, LDD01 produced a model for the HTCs with 4 free parameters and then determined which of these models were consistent with the orbital element distribution of the observed HTCs. There are two free parameters that define the structure of the Oort cloud. The parameter i' is the median inclination of the inner Oort cloud, which is defined to have $a < 20,000$ AU. The outer part of the Oort cloud is assumed to be isotropic. The parameter w_{out} is a measure of the relative mass of the inner and outer parts. The larger w_{out} is, the more mass the outer cloud has with respect to the inner. There is one free parameter that describes the bias against finding active comets with large semi-major axes, P_{cut}. In these models, the probability of discovering a comet is 1 if its orbital period (P) is less than P_{cut} and the probability is P/P_{cut} if $P > P_{cut}$. There is one parameter to account for the fading of comets. The parameter N_q is the number of perihelion passages that a comet will undergo before it fades. See LDD01 for a complete definition.

LDD01 found quite a number of models that were consistent with the observed distribution of active HTCs. Their best fit model had $i' = 20°$, $P_{cut} = 30$ years, $N_q = 5000$ passages, and $w_{out} = 0.001$. A 2-dimensional Kolmogorov-Smirnov (K-S) test [7] on inclinations and semi-major axes shows that the probability that the model distribution and real distribution are derived from the same parent distribution is 0.6. Thus, the fit is good. However, there are reasons to distrust these models. First, they predict a massive flattened inner Oort cloud, which seems inconsistent with current models of Oort cloud formation [8]. In addition, they predict a dynamically active flattened inner cloud (meaning that it is currently feeding comets directly to Saturn). It is difficult to understand how this structure could be this dynamically active and yet remain flattened. Thus, we believe that

there are problems in our understanding of the origin of the HTCs. Despite this, the LDD01 models are the best in existence and most likely produce a reasonable orbital element distribution for the HTCs. Thus, we adopt a modified version of LDD01's models (see next section) for this paper.

For the models presented here, we employed LDD01's fitting procedures to find the best fit to both the active and dormant HTC populations, assuming $\alpha = 0.28$ (however, see below). As in LDD01, for each model, we calculated the probability that the Semi-major axis – inclination (a–i) distribution of the model was drawn from the same population as the observed a–i distribution using a 2-dimensional K-S test. We did this for the active and dormant comets independently. Our best fit model, which we defined as that model with the largest product of the active and dormant K-S probabilities, has $i' = 20°$, $P_{cut} = 20$ years, $N_q = 20000$ passages, and $w_{out} = 0.004$. For this model the active and dormant K-S probabilities were 0.74 and 0.75, respectively.

As described in the main body of this paper, this model predicts that there should be $\sim$ 106,000 HTCs with $q < 2.5\,\mathrm{AU}$. Because dormant comets far outnumber the active comets, this result implies that $\sim 99\%$ of ERCs disrupt before becoming HTCs. This percentage is similar to the fraction predicted for the ERCs alone. The similarity between HTCs and ERCs is not surprising because the best fit model's $N_q = 20,000$ is larger than the average number of perihelion passages an HTC experiences in our models assuming no physical evolution (~ 1800). Thus, there is very little fading while comets are HTCs. This outcome implies that all the fading (whether via dormancy or disruption) must happen before comets become HTCs.

V. Justification for a Disruption Law that is Dependent on q: In order to build HTC models that match the observations, we adopted a model in which: *i*) if an object evolves onto an orbit with $q < 1\,\mathrm{AU}$, we assume that it has a 96% chance of disrupting before its next perihelion passage (i.e. it is visible this passage, but disappears before the next), *ii*) if the comet disrupts then it will not appear in either the active comet or dormant comet populations, and *iii*) if it survives the

first $q < 1$ AU passage, it will survive forever as an active or dormant object. We believe our scenario is reasonable because [9] showed that periodic comets that have recently undergone large reductions of their perihelion distances typically are most affected by nongravitational forces. Since these forces are caused by the comet's activity, an increase in nongravitational force probably implies a larger cometary erosion rate. A model where we remove objects with $q < 1$ AU is the simplest way to invoke this hypothesis.

We justify this removal criterion by noting that 1) there is an observed dearth of ERCs with small perihelion distances compared to dynamically new comets [10,11], and 2) other investigators have inferred that Halley-type comets with smaller q survive for a smaller number of orbits [12] However, we cannot remove *all* objects with $q < 1$ AU because several of the known active HTCs have perihelion distances smaller than this and have undergone multiple perihelion passages (most notably, 1P/Halley; see [13] for a list of HTCs with $q < 1$ AU). So, we adopt one of the fading laws suggested by WT99 for active ERCs: 96% of comets fade very quickly (which we take to mean in the first passage), while the remaining 4% live forever.

The result that LDD01's models require a disruption law that is a function of q can place constraints on the population of asteroids from the main belt that reside in the Oort cloud. It has been argued [14] that $\sim 1\%$ on the objects in the Oort cloud originated in the asteroid belt. Indeed, 1996 PW has a $\sim 50\%$ chance of being an Oort cloud object that originated in the asteroid belt [14]. Oort-cloud asteroids will not contribute to the active comet population, but will contribute to what we are calling dormant NICs. However, we assume they will not disrupt, whatever their orbital history, because they are primarily rocky bodies. Thus, the need to add an orbit-dependent disruption to our models to match the semi-major axis distribution of the dormant HTCs implies that asteroids cannot significantly contribute to this population. Therefore, much less than 1% of the Oort cloud originated in the asteroid belt.

VI. Note on Disruption: We have demonstrated that the population of dormant nearly-isotropic comets with $H < 18$ is about 1% of that predicted in our models

without disruption. This implies that either the comets break apart into small, undetected pieces, or the albedo of the objects is much smaller than the already low values we have assumed. To quantify these possibilities, we have run the survey simulator on populations with increasingly faint limiting absolute magnitudes and have taken smearing into account (See §1 of the SOM).

Using the 2 detections of dormant ERCs (Table 1), we estimate that there are 44,000 ERCs with $H < 18$ (call this N_{obs}). If comets did not disintegrate and had an albedo that was independent of the comet's size, the model of WT99 implies that there should be 4.4×10^6 dormant ERCs with $H < 18$ (call this N_{mod}). In order for the differences between model and observations to be caused by dormant comets having a much smaller albedo than we assume,

$$N_{obs}(H < 18) = N_{mod}(H < 18) \left(\frac{p_{mod}}{p_{obs}} \right)^{-2.5\alpha},$$

where p_{mod} is the albedo we assume in our model and p_{obs} is the albedo comets must have to account for the differences between the models and observations. Using our assumed values of $p_{mod} = 0.02$ [15] and $\alpha = 0.28$, we find that $p_{obs} = 3 \times 10^{-5}$. Because surfaces this dark have never been observed in the solar system, we reject this possibility and conclude that comets must break apart.

Given that comets disrupt, we can estimate the maximum size of the fragments that resulted from the disruption. If we assume that the size distribution of the fragments is steep, there will be one large fragment for each disrupted comet. In addition, if we assume that these fragments are the same size independent of the original size of the comet, the resulting large fragments must be faint enough so that a population of 4.4×10^6 would not be discovered by our surveys. We find that this occurs for objects fainter than $H = 19.5$ (at the 90% confidence level), which corresponds to an object with a diameter of ~ 1.2 km. We point out, however, that the assumption that the largest fragments are all the same size probably is not realistic.

We can also assume that the largest fragment is a fixed fraction of the comet's original size, so that $H_{frag} = H_{comet} + dH$, where H_{frag} and H_{comet} are the absolute

magnitude of the fragment and the original comet, respectively. Assuming the 44 million comets predicted by WT99 model have $12 < H < 18$, in order to have only 44,000 fragments with $H < 18$, dH must be 5.4. If the original population of comets extends to $H < 12$, dH must be even larger. A dH of 5.4 implies that the diameter of the largest fragment of a breakup is 1/12 of the diameter of the original comet. If we naively apply this to a $H = 18$ comet, we find that the largest fragment has a diameter of 200m, assuming a 2% albedo. However, a 200m object has $H = 23$, which, as we described in §I of this SOM, is below the detection threshold of the surveys ($H \sim 22$). Therefore, there are no real observational constraints on objects this small. An object near the detection threshold has a diameter of $\sim$ 400 m assuming a 2% albedo. This size is a more reasonable upper limit for the diameter of the fragments.

Thus, in this manuscript we use the verb 'disrupt' in the sense of 'breaking up into pieces in which the largest fragments are smaller than a few 100 meters.' It should be noted, however, that the disruption of Comet C/1999 S4 (LINEAR) suggests that the largest fragments are only tens of meters in size [16].

VII. Impact Rates on the Earth: Our calculations of the number and orbits of dormant NICs allows us to estimate the impact rates of these objects with the Earth. Again, we must divide NICs into ERCs and HTCs. Assuming the orbital element distribution given by WT99 [3], we estimate that Earth suffers one impact every 370 My from a $H < 18$ dormant ERC, using methods described in [17]. For the HTCs, we conclude that there are 780 ± 260 dormant HTCs in the solar system with $H < 18$ and $q < 2.5$ AU. This corresponds to an Earth impact rate of one $H < 18$ dormant HTC per 840 My. Since both these impact rates are much smaller than that of the NEO's, which is one $H < 18$ object per 0.5 Myr [18], we can conclude that dormant NICs currently do not represent a significant fraction of the hazard to Earth. This conclusion may not apply at all times because it assumes that NICs are in steady state. Indeed, it may not be true during comet showers [19].

VIII. Disruption of Jupiter-family comets: In the main portion of this paper, we conclude based on our modeling that dynamical models of the JFCs predict $\sim$ 105 assuming no disruption while observations show that there are 61 ± 43. Thus, we argue that a significant fraction of the JFCs survive. We can arrive at a similar conclusion if we estimate the amount of material in the JFC's source regions assuming a 99% disruption rate. The active JFCs originate in either the Kuiper belt [20, 21] or the scattered disk [22]. If the JFCs originate in the Kuiper belt and there is no physical disruption, then the Kuiper belt must contain $\sim 7 \times 10^9$ comet-sized objects [21]. However, if we assume that the disruption rate for the JFCs is the same as we found for the ERCs (i.e. 99% disrupt) then the Kuiper belt must contain $7 \times 10^9 \times 100 = 7 \times 10^{11}$ comets. Using an average cometary mass of 3.8×10^{16} g [4], this implies that the Kuiper belt must contain at least $4M_\oplus$ of material in its inner regions (the ones that supply the JFCs). This is inconsistent with current constraints on the Kuiper belt [23]. If we assume that the scattered disk is the source of the JFCs, then assuming a 99% disruption rate implies that the must be $6 \times 10^8 \times 100 = 6 \times 10^{10}$ or $0.4M_\oplus$ in the scattered disk. This again is more material than could be there [22,23]. Thus, we can conclude again that the JFCs do not suffer disruption at the same rate as the NICs.

References

[1] G. H. Stokes *et al.*, *Icarus* **148**, 21 (2000).

[2] R. Jedicke, Morbidelli, A., Spahr, T., Petit, J-M., & Bottke W, *Icarus*, submitted (2002).

[3] P. Wiegert, S. Tremaine, *Icarus* **137**, 84 (1999), hereafter WT99.

[4] P. R. Weissman, in *Global Catastrophes in Earth History*, V. L. Sharpton and P. D. Ward, Eds. (Geological Soc. of America Special Pap. 247, 1990), 171.

[5] M. A. Bailey and C. R. Stagg, *Mon. Not. R. Astron. Soc.* **235**, 1 (1988).

[6] H. F. Levison, L. Dones, M. J. Duncan, *Astron. J.* **121**, 2253 (2001), hereafter LDD01.

[7] W. H. Press, S. A. Teukolsky, W. T. Vetterling, and B. P. Flannery, *Numerical Recipes in FORTRAN*, 2nd Ed., Cambridge Univ. Press, p. 640 (1992)

[8] L. Dones,H. Levison,M. Duncan,and P. Weissman, *Bull. Amer. Astron. Soc.* **32**, abstract #36.02 (2000);
`http://www.boulder.swri.edu/~luke/oort.html`.

[9] H. Rickman, L. Kamél, Cl. Froeschlé, M. Festou (*Astron. J.* **102**, 1446 (1991)

[10] P. R. Weissman, in *Comets*, ed. L. L. Wilkening, (Univ. Arizona Press, 1982), p. 637

[11] P. R. Weissman, in *Dynamics of the Solar System*, IAU Symposium 81, R. L. Duncombe, Ed. (Reidel, Dordrecht, 1979), p. 277.

[12] V. V. Emel'yanenko and M. E. Bailey (*Mon. Not. R. Astron. Soc.* **298**, 212 (1998)

[13] E. M. Shoemaker, P. R. Weissman, C. S. Shoemaker, in *Hazards due to Comets and Asteroids*, T. Gehrels, Ed. (Univ. Arizona Press, 1994), 317.

[14] P. R. Weissman and H. F. Levison, *Astrophys. J. Lett.* **488**, 133 (1997).

[15] Y. R. Fernández, D. C. Jewitt, & S. S. Sheppard, *Ap. J. Lett.* **553**, L197 (2001).

[16] H. Boehnhardt, *Science* **292**, 1307 (2001).

[17] W. F. Bottke, M. C. Nolan, R. Greenberg, and R. A. Kolvoord, *Icarus* **107**, 255 (1994).

[18] A. Morbidelli, W. F. Bottke, Ch. Froeschlé, and P. Michel, to appear in *Asteroids III* (W. F. Bottke, A. Cellino, P. Paolicchi, R. Binzel, Eds.), U. Arizona Press, in press (2002).

[19] J. G. Hills, *Astron. J.* **86**, 1730 (1981).

[20] M. Duncan, T. Quinn, and S. Tremaine, *Astphy. J. Lett.* **328**, 69 (1988).

[21] H. F. Levison, M. J. Duncan, *Icarus* **127**, 13 (1997).

[22] M. J. Duncan, H. F. Levison, *Science* **276**, 1670 (1997).

[23] C. A. Trujillo, D. C., Jewitt, & J. X. Luu, *Astrophy. J. Lett.* **529**, 103 (2000).

Fig. S1 — The cumulative semi-major axis (a) distribution of external returning comets (ERCs). The solid curve shows the intrinsic distribution as predicted by WT99. The dotted curve shows the a distribution of the ERCs that should be discovered by the NEO surveys as predicted by our survey simulator.

Fig. S2 — The probability ($P_{\rm KS}$) that the absolute magnitude distribution of our modeled dormant HTCs and that of real dormant HTCs are derived from the same parent distribution. This probability was determined using a 1-dimensional K-S test.

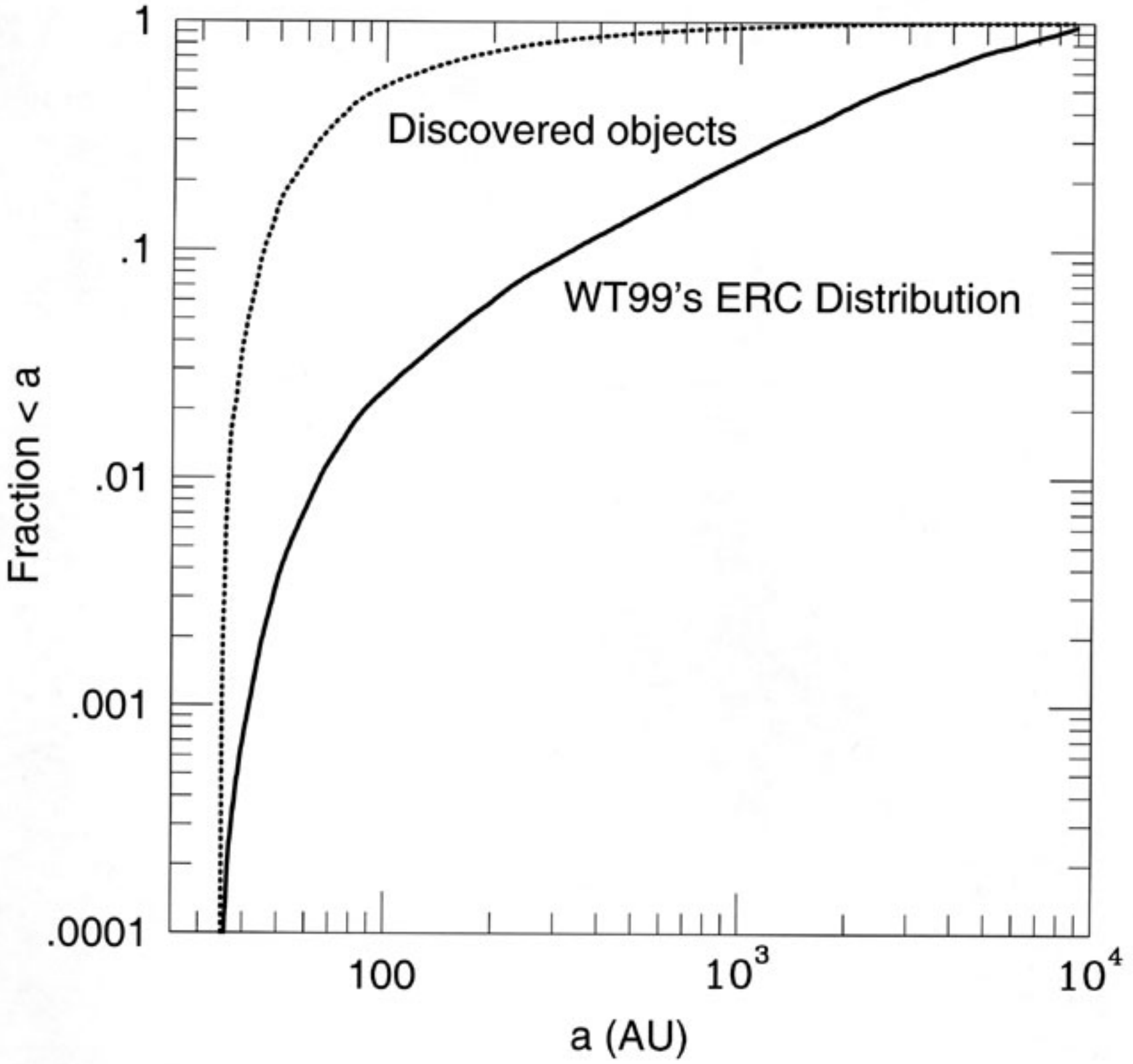
1
.1
.01
.001
.0001
Fraction < a
Discovered objects
WT99's ERC Distribution
100
10^3
10^4
a (AU)

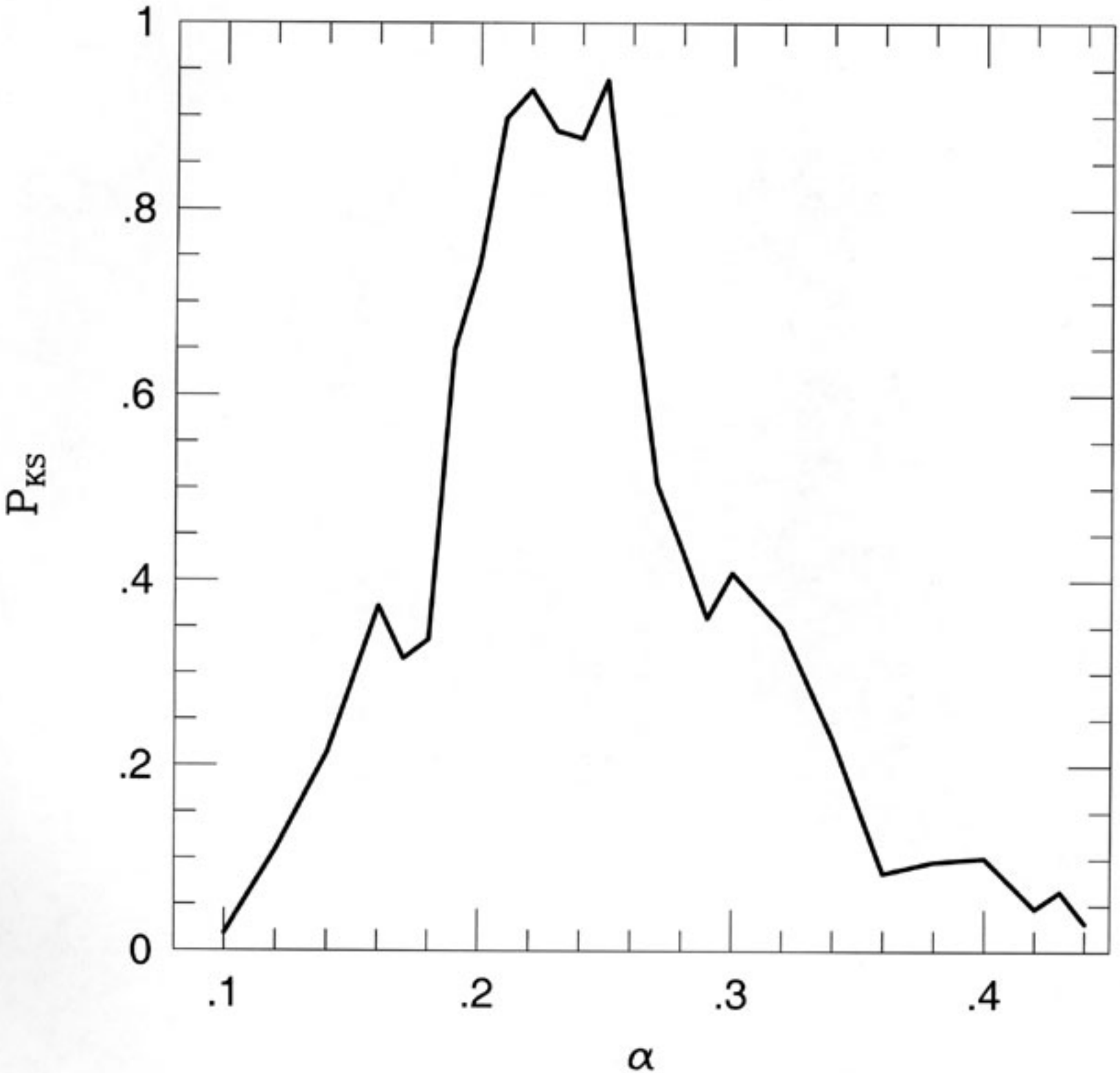
1
.8
.6
.4
.2
0
P_{KS}
.1
.2
.3
.4
α